Electronic Supplementary Material (ESI) for Physical Chemistry Chemical Physics.

Supporting Information for

Elucidating Electrolyte Decomposition under Electron-Rich Environments at the Lithium-Metal Anode

Luis E. Camacho-Forero[1] and Perla B. Balbuena[1,2,3,*]

[1]Department of Chemical Engineering, [2]Department of Materials Science and Engineering, [3]Department of Chemistry, Texas A&M University, College Station, TX 77843

*e-mail: balbuena@tamu.edu

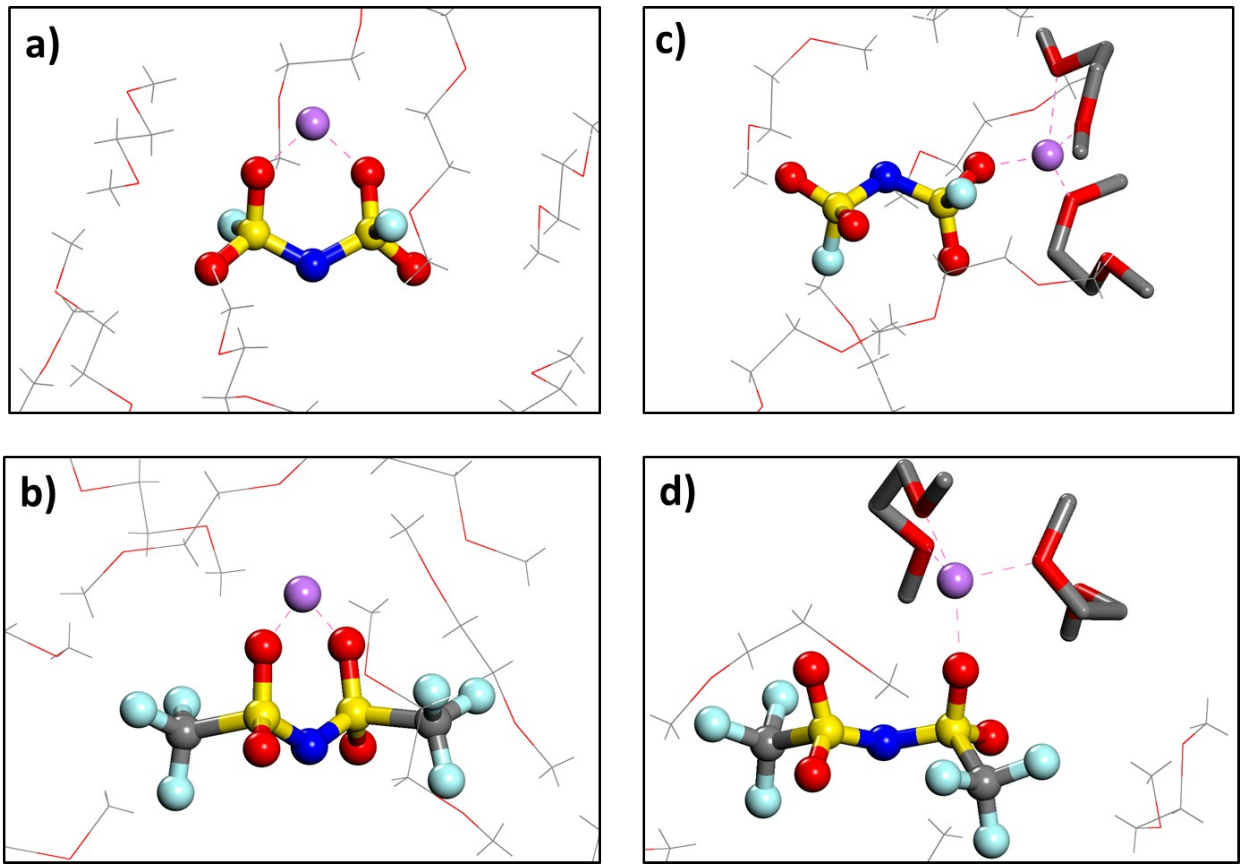

Figure S1. Initial configurations of 1M solutions for AIMD simulations under electron-rich environments. (a-b) MM-relaxed and (c-d) AIMD-relaxed initial configurations. Color code as in Figure 1.

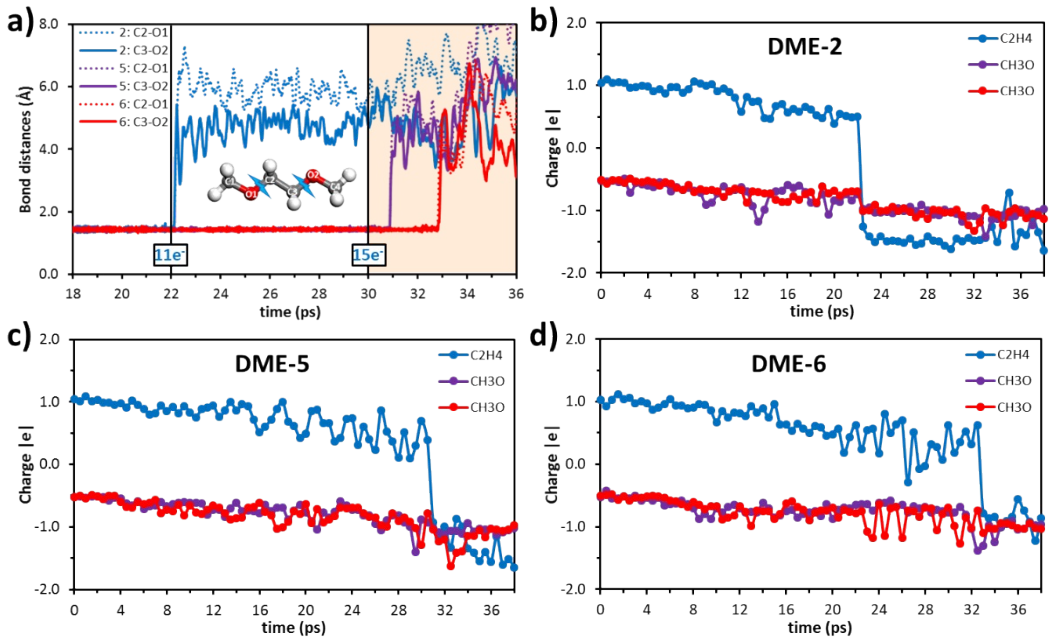

Figure S2. DME reaction mechanism from AIMD simulations of pure DME with sequential addition of electrons. (a) C-O bond distances for reacting DME molecules. (b-d) Charges evolution of fragments from reacting DME molecules. Color code as in Figure 1.

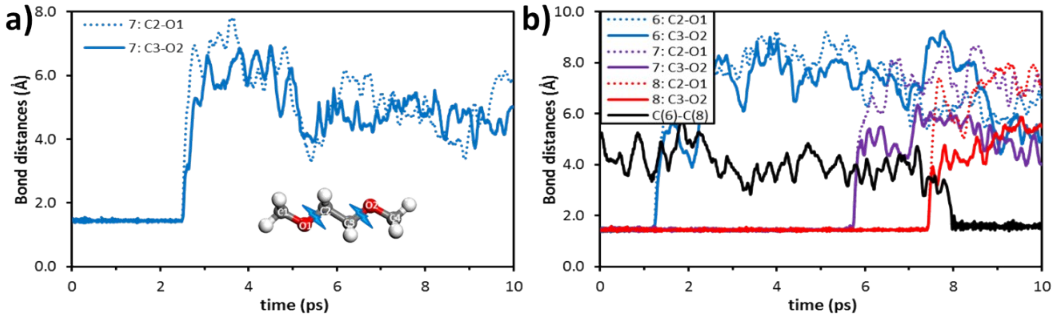

Figure S3. Bond distance evolution for DME molecules from AIMD simulations of pure solvent with constant number of excess electrons starting with the MM-relaxed initial configuration. (a) n_{eo}=11 and (b) n_{eo}=13 – also includes the C-C bond distance for the oligomer $(C_2H_4)_2^{2-}$.

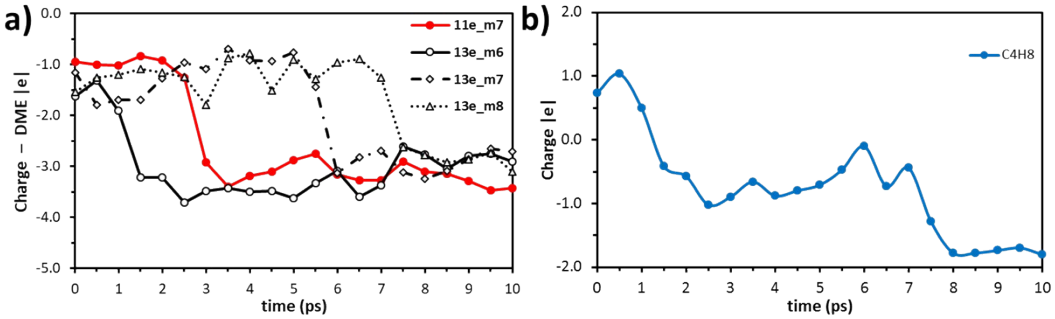

Figure S4. Charge evolution of (a) reacting DME molecules and (b) $(C_2H_4)_2^{2-}$ from AIMD simulations of pure solvent with constant number of excess electrons starting with the MM-relaxed initial configuration.

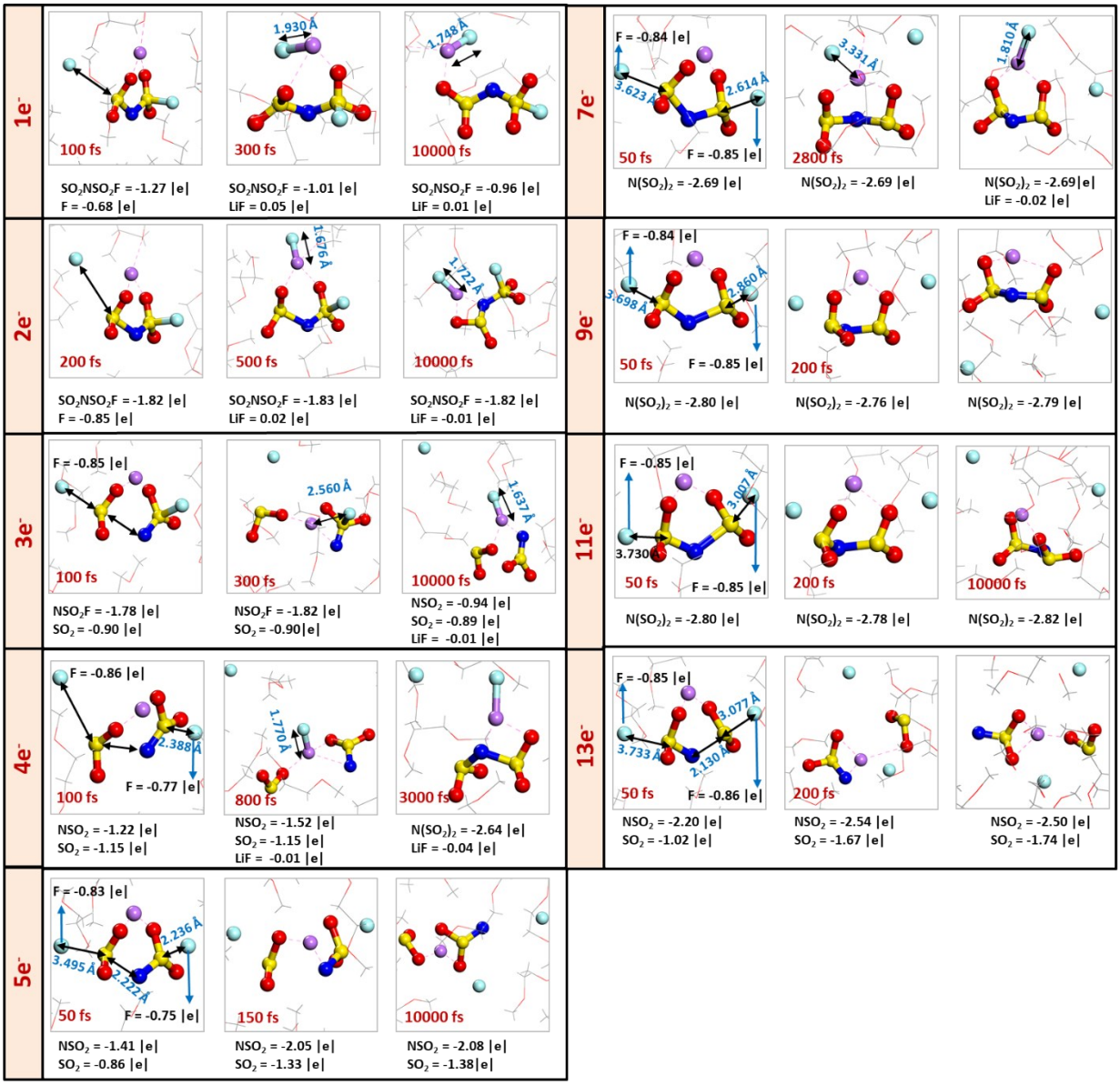

Figure S5. LiFSI reduction mechanism from AIMD simulations of 1M LiFSI solutions with various number of excess electrons (n_{eo}) starting with the MM-relaxed initial configuration. Color code as in Figure 1.

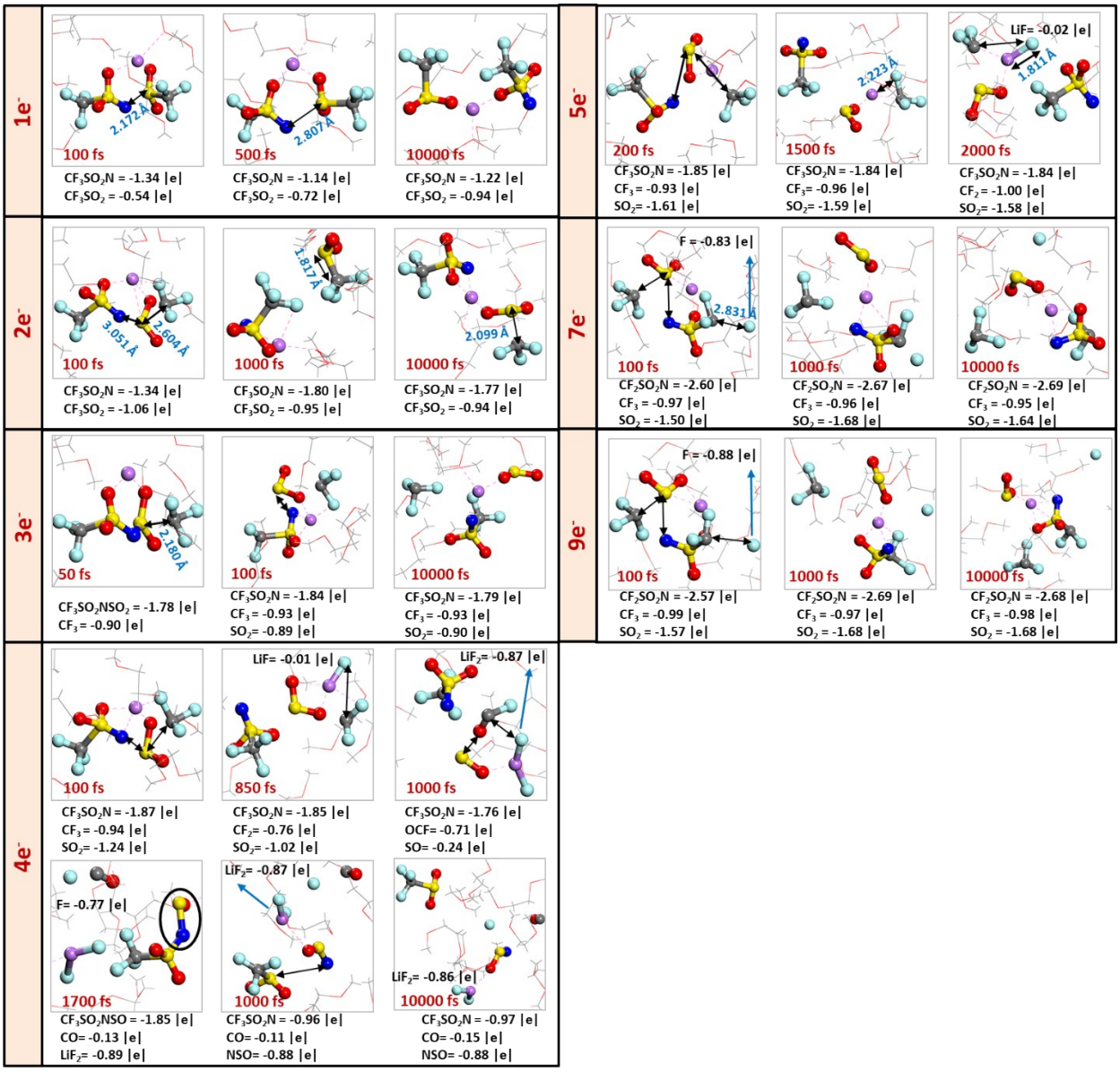

Figure S6. LiTFSI reduction mechanism from AIMD simulations of 1M LiFSI solutions with various number of excess electrons (n_{eo}) starting with the MM-relaxed initial configuration. LiTFSI reduction involving DME redox reactions (n_{eo}= 11 and 13) are shown in Figure 7. Color code as in Figure 1.

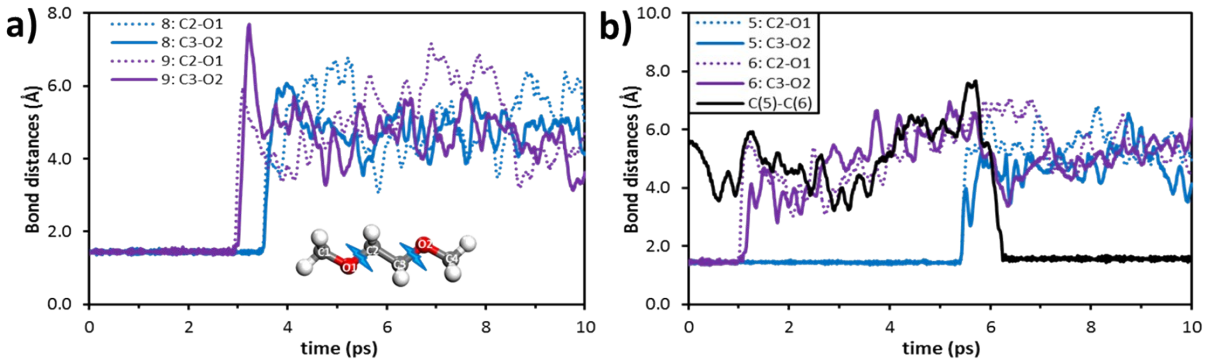

Figure S7. Bond distance evolution for DME molecules from AIMD simulations of pure solvent with constant number of excess electrons starting with the AIMD-relaxed initial configuration. (a) n_{eo}=11 and (b) n_{eo}=13 – also includes the C-C bond distance for the oligomer $(C_2H_4)_2^{2-}$.

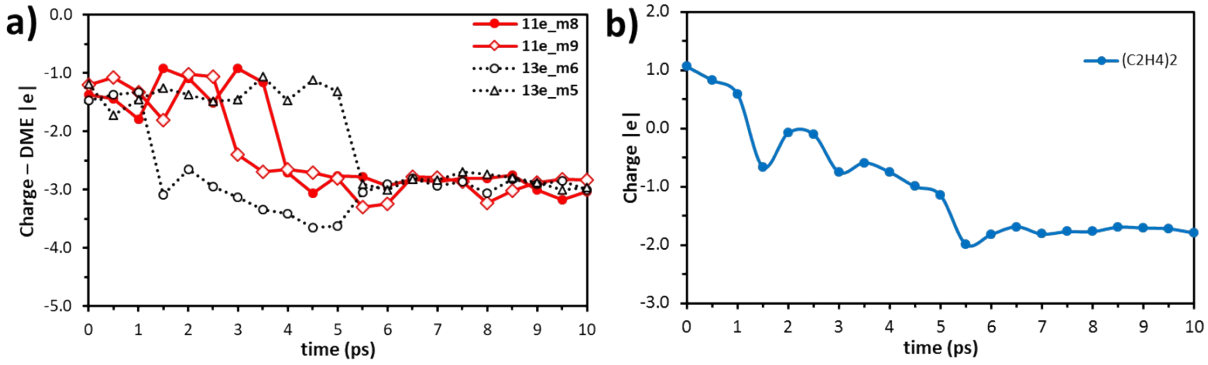

Figure S8. Charge evolution of (a) reacting DME molecules and (b) $(C_2H_4)_2^{2-}$ from AIMD simulations of pure solvent with constant number of excess electrons starting with the AIMD-relaxed initial configuration.

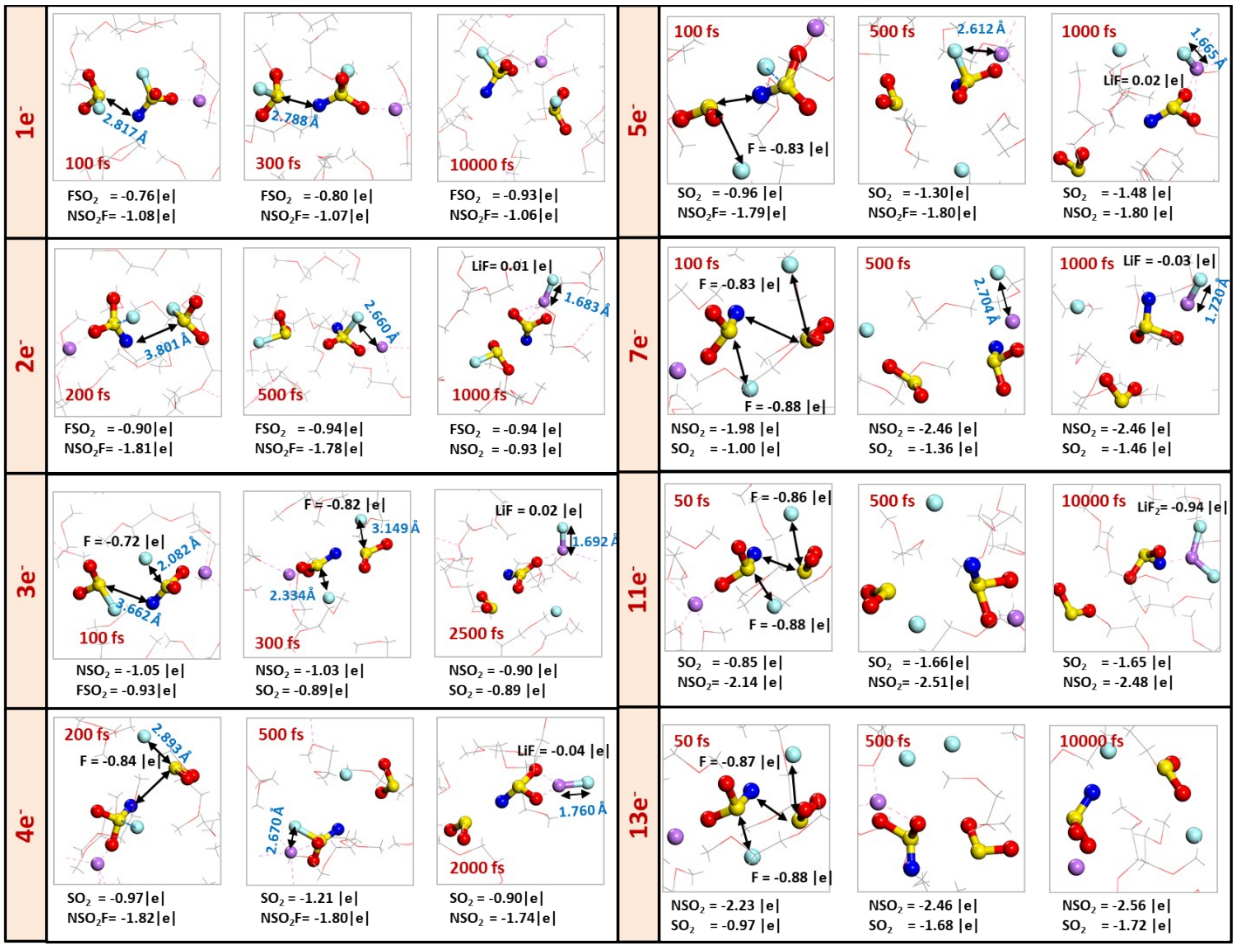

Figure S9. LiFSI reduction mechanism from AIMD simulations of 1M LiFSI solutions with various number of excess electrons (n_{eo}) starting with the AIMD-relaxed initial configuration. LiFSI reduction involving DME redox reactions (n_{eo}= 9) are shown in Figure 9a. Color code as in Figure 1.

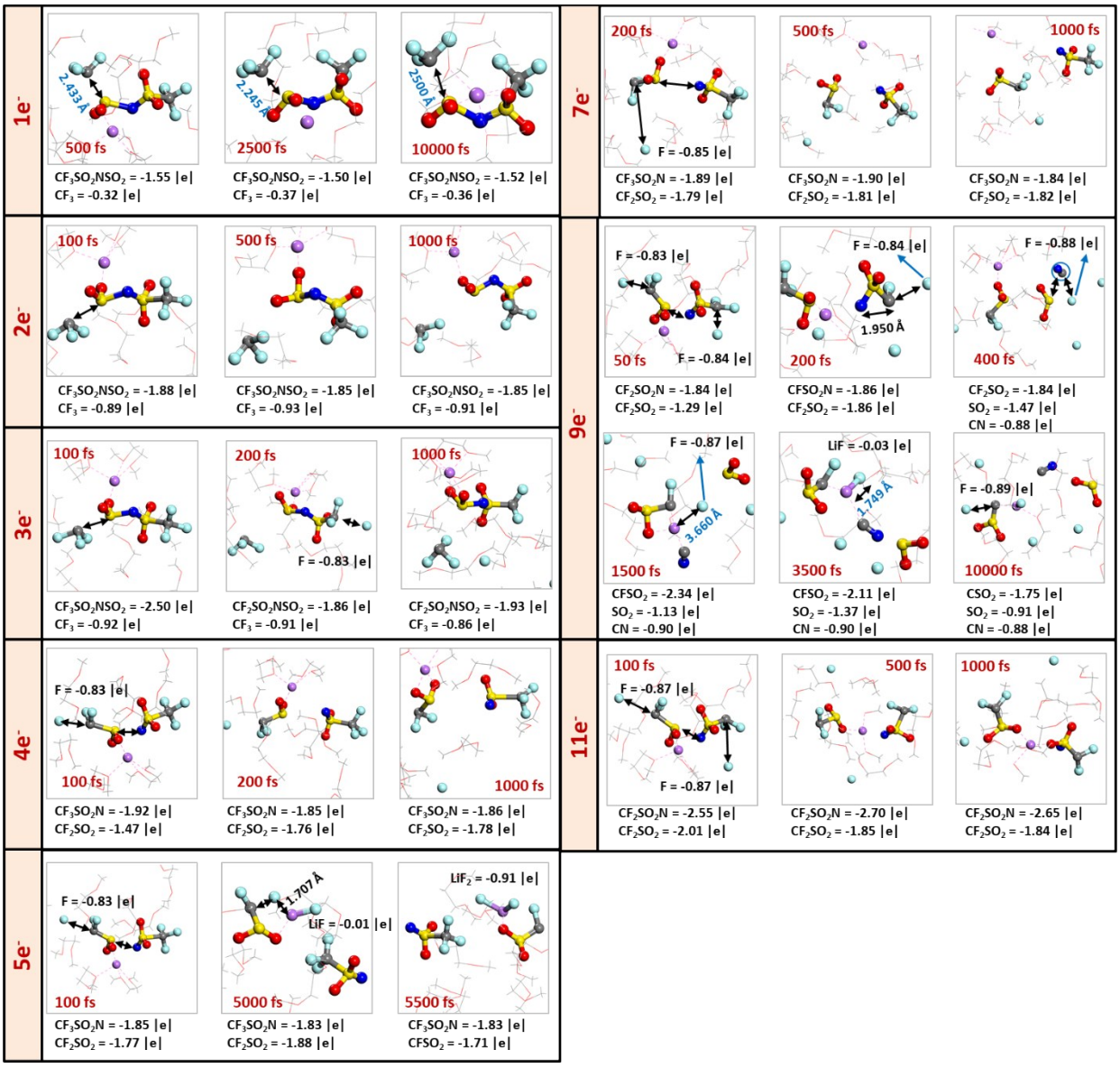

Figure S10. LiTFSI reduction mechanism from AIMD simulations of 1M LiTFSI solutions with various number of excess electrons (n_{eo}) starting with the AIMD-relaxed initial configuration. LiTFSI reduction involving DME redox reactions (n_{eo}= 13) are shown in Figure 9b. Color code as in Figure 1.

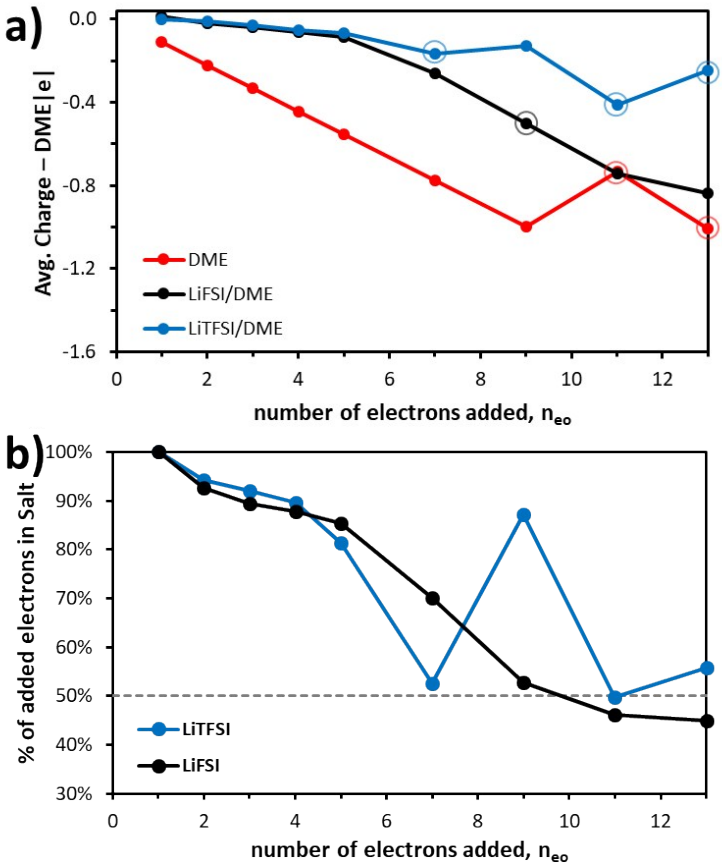

Figure S11. Average Charges over 10 ps of AIMD in solutions starting with AIMD-relaxed configuration (sampled every 1 ps) as a function of the initial number of excess electrons. (a) Average charges of non-reacting DME. Circles indicate systems where reactions took place. (b) Percentage of added electrons accepted by the salts. The dotted line depicts the 1:1 electron distribution between salt and solvent.

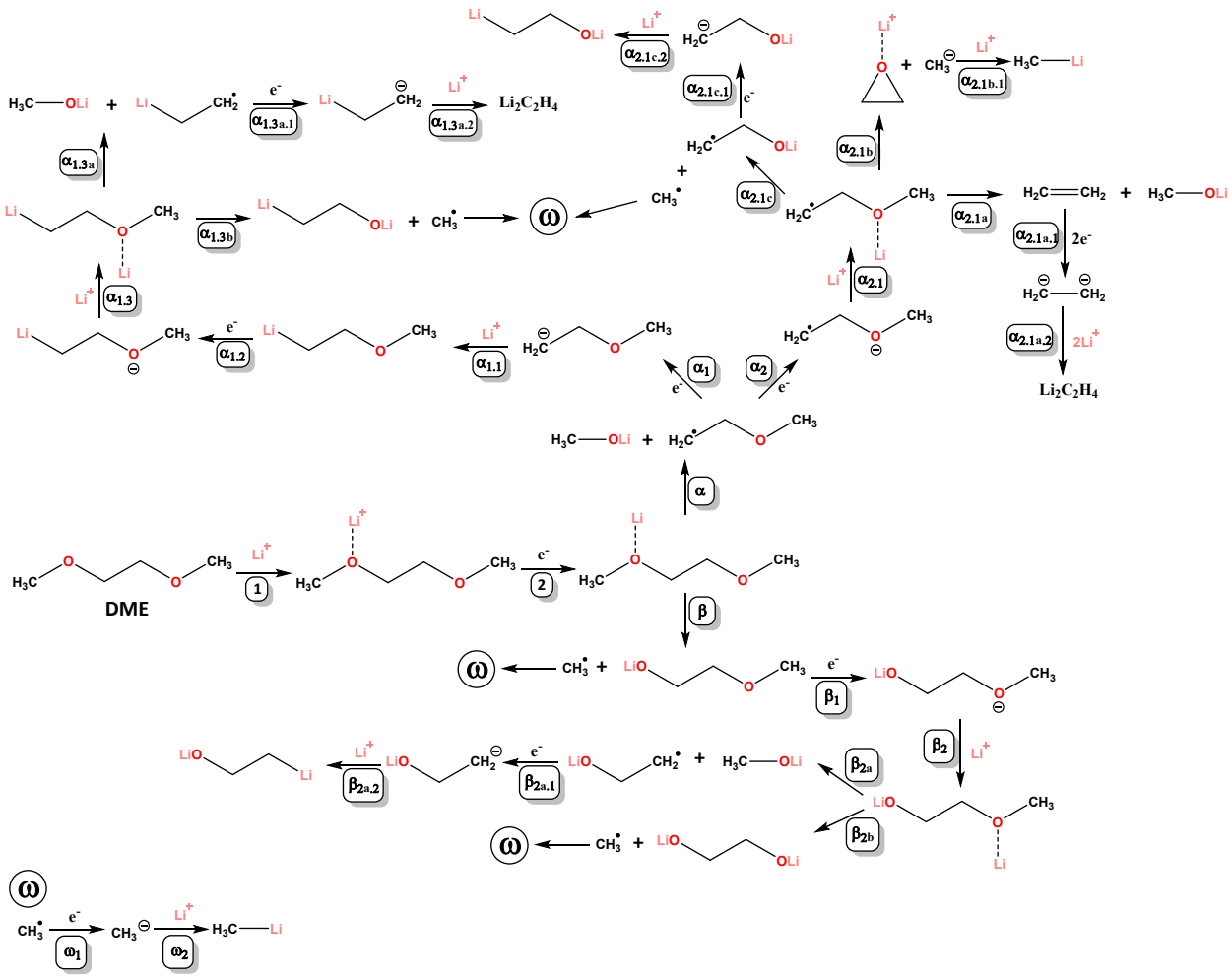

Figure S12. All possible reaction pathways for DME decomposition under one Li-radical attack yielding C-O bond scission.

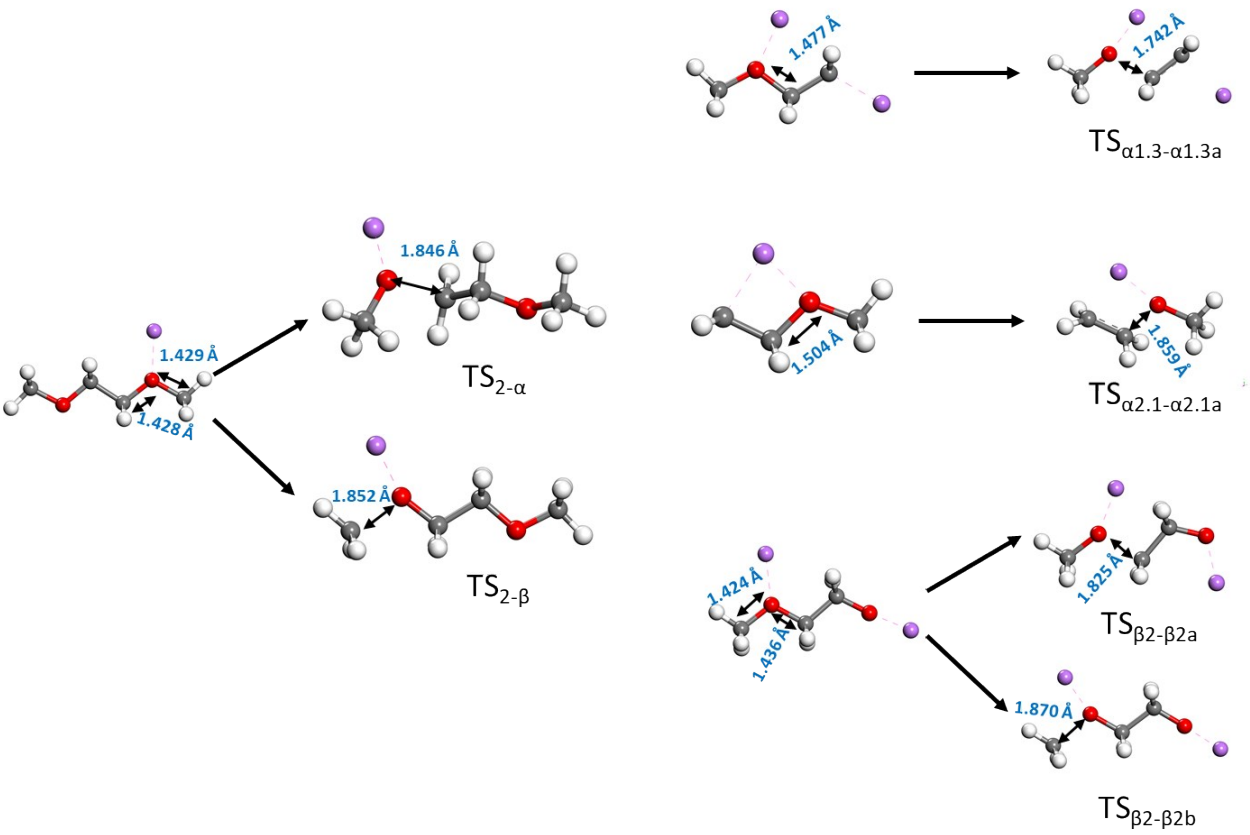

Figure S13. Intermediates and transition states structures calculated from B3PW91/6-311++G(p,d). Color code as in Figure 1. Refer to Figure 10 for reactions numbering.

Table S1. Calculated electron affinity (EA) for electrolyte components from B3PW91/6-311++G(p,d) in solvent (DME).

Molecule	E(0) (eV)	E(-1) (eV)	EA (eV)
DME (TTT)	-308.70	-308.71	-0.25
DME (TGT)	-308.70	-308.71	-0.27
LiFSI	-1359.08	-1359.13	-1.44
LiTFSI	-1834.59	-1834.64	-1.35

Table S2. Summary of bond cleavage and fragments remaining after 10 ps of AIMD simulation in 1M solutions with AIMD-relaxed initial configurations. Structures in red are species neutrally charged. "Fragments w/ DME" makes allusion only to DME molecules decomposed due to a salt fragment.

number of electrons	LiFSI			LiTFSI		
	Initial Bond Cleavages	Salt fragments	fragments w/ DME	Initial Bond Cleavages	Salt fragments	fragments w/ DME
1	S-N	FSO_2, NSO_2F	-	C-S	CF_3--$SO_2NSO_2CF_3$	-
2	S-N, S-F	FSO_2, NSO_2, LiF	-	C-S	CF_3, $SO_2NSO_2CF_3$	-
3	S-N, S-F, S-F	SO_2, NSO_2, LiF, F^-	-	C-S, C-F	CF_3, $SO_2NSO_2CF_2$, F^-	-
4	S-N, S-F, S-F	SO_2, NSO_2, LiF, F^-	-	S-N, C-F	CF_2SO_2, NSO_2CF_3, F^-	-
5	S-N, S-F, S-F	SO_2, NSO_2, LiF, F^-	-	S-N, C-F, C-F	$CFSO_2$, NSO_2CF_3, LiF_2^-	-
7	S-N, S-F, S-F	SO_2, NSO_2, LiF, F^-	-	S-N, C-F	CF_2SO_2, NSO_2CF_3, F^-	-
9	S-N, S-F, S-F	SO_2, NSO_2, $2F^-$	$HNSO_2$, $CH_3O(CH_2)_2OCH_2^-$	S-N, C-F, C-F	SO_2, NC, CSO_2, LiF, $4F^-$	-
11	S-N, S-F, S-F	SO_2, NSO_2, LiF_2^-	-	S-N, C-F, C-F	CF_2SO_2, NSO_2CF_2, $2F^-$	-
13	S-N, S-F, S-F	SO_2, NSO_2, $2F^-$	-	S-N, C-F, C-F	CF_2SO_2, CSO_2N, $4F^-$	$HCSO_2N$, CH_3O^-, CH_3OCHCH_2

Table S3. Calculated bond dissociation energies for DME from B3PW91/6-311++G(p,d) in solvent (DME).

Bond	ΔE_0 (eV)	ΔG_{298} (eV)
C_m-H_m	4.36	4.25
C_t-H_t	4.85	4.76
C_m-O	4.56	4.41
O-C_t	5.08	4.89

Table S4. Calculated reaction energies and activation barriers for DME under one-lithium radical attack from B3PW91/6-311++G(p,d) in solvent (DME).

Reaction	Reaction Energy (eV)				
	ΔE	ΔE_{0K}	ΔE_{298K}	ΔH_{298K}	ΔG_{298K}
1	-0.70	-0.63	-0.63	-0.65	-0.36
2	-1.90	-1.92	-1.92	-1.92	-1.94
α	-0.12	-0.38	-0.33	-0.33	-0.56
α_1	-2.67	-2.69	-2.69	-2.69	-2.68
$\alpha_{1.1}$	-1.94	-1.87	-1.87	-1.89	-1.58
$\alpha_{1.2}$	-1.21	-1.23	-1.23	-1.23	-1.25
$\alpha_{1.3}$	-0.74	-0.68	-0.71	-0.71	-0.45
$\alpha_{1.3a}$	-0.63	-0.82	-0.78	-0.78	-0.98
$\alpha_{1.3a.1}$	-1.06	-1.12	-1.12	-1.12	-1.10
$\alpha_{1.3a.2}$	-2.35	-2.27	-2.28	-2.30	-1.96
$\alpha_{1.3b}$	0.57	**0.30**	0.36	0.36	**0.12**

α_2	-2.67	-2.69	-2.69	-2.69	-2.68
$\alpha_{2.1}$	-2.31	-2.22	-2.23	-2.25	-1.92
$\alpha_{2.1a}$	-0.52	-0.64	-0.62	-0.60	-1.09
$\alpha_{2.1a.1}$	-0.69	-0.85	-0.84	-0.84	-0.89
$\alpha_{2.1a.2}$	-5.41	-5.26	-5.28	-5.33	-4.68
$\alpha_{2.1b}$	2.68	**2.50**	2.53	2.55	**2.06**
$\alpha_{2.1c}$	4.25	**3.92**	3.89	3.89	**3.85**
$\alpha_{2.1c.1}$	-2.15	-2.16	-2.18	-2.18	-2.09
$\alpha_{2.1c.2}$	-2.11	-2.06	-2.05	-2.08	-1.81
β	-0.12	-0.40	-0.34	-0.34	-0.56
β_1	-1.24	-1.25	-1.25	-1.25	-1.28
β_2	-0.49	-0.44	-0.47	-0.47	-0.24
β_{2a}	0.03	-0.21	-0.13	-0.13	-0.53
$\beta_{2a.1}$	-2.15	-2.16	-2.18	-2.18	-2.09
$\beta_{2a.2}$	-2.11	-2.06	-2.05	-2.08	-1.81
β_{2b}	0.10	-0.16	-0.11	-0.11	-0.30
ω_1	-2.68	-2.69	-2.70	-2.70	-2.67
ω_2	-2.06	-1.97	-1.99	-2.01	-1.72
$TS_{2-\alpha}$	1.05	0.88	-	-	0.86
$TS_{\alpha1.3-\alpha1.3a}$	0.04	**-0.01**	-	-	**-0.02**
$TS_{\alpha2.1-\alpha2.1a}$	0.10	0.05	-	-	0.04
$TS_{2-\beta}$	0.97	0.80	-	-	0.75
$TS_{\beta2-\beta2a}$	1.04	0.90	-	-	0.92
$TS_{\beta2-\beta2b}$	1.09	0.94	-	-	0.94

Table S5. Calculated reaction energies and activation barriers for DME decomposition via dehydrogenation due to anion attack from B3PW91/6-311++G(p,d) in solvent (DME).

Step	H_m+O--LiF		H_t+O--LiF	
	ΔE_{0K}	$\Delta G_{298.15K}$	ΔE_{0K}	$\Delta G_{298.15K}$
TS_1	-0.22	**0.24**	-0.13	**0.31**
1	-1.47	-1.48	-1.30	-1.31
TS_{1-2}	0.08	**0.08**		
2	-0.86	-1.34		
TS_{1-3}	0.19	**0.67**		
3	-1.50	-1.52		